minerals

MDPI

Article

Mineralogy and Geochemistry of Biologically-Mediated Gold Mobilisation and Redeposition in a Semiarid Climate, Southern New Zealand

Gemma Kerr and Dave Craw *

Geology Department, University of Otago, P.O. Box 56, Dunedin 9054, New Zealand; gemma.kerr@otago.ac.nz
* Correspondence: dave.craw@otago.ac.nz; Tel.: +64-3-479-7529

Received: 21 July 2017; Accepted: 13 August 2017; Published: 16 August 2017

Abstract: Detrital gold in Late Pleistocene-Holocene placers has been chemically mobilised and redeposited at the micron scale by biologically-mediated reactions in groundwater. These processes have been occurring in a tectonically active semiarid rain shadow zone of southern New Zealand and are probably typical for this type of environment elsewhere in the world. The chemical system is dominated by sulfur, which has been derived from basement pyrite and marine aerosols in rain. Detrital and authigenic pyrite is common below the water table, and evaporative sulfate minerals are common above the fluctuating water table. Pyrite oxidation was common but any acid generated was neutralised on the large scale (tens of metres) by calcite, and pH remained circumneutral except on the small scale (centimetres) around pyritic material. Metastable thiosulfate ions were a temporary product of pyrite oxidation, enhanced by bacterial mediation, and similar bacterial mediation enhanced sulfate reduction to form authigenic pyrite below the water table. Deposition of mobilised gold resulted from localised variations in redox and/or pH, and this formed overgrowths on detrital gold of microparticulate and nanoparticulate gold that is locally crystalline. The redeposited gold is an incidental byproduct of the bacterially-enhanced sulfur reactions that have occurred near to the fluctuating sulfide-sulfate redox boundary.

Keywords: gold; pyrite; sulfate; groundwater; geomicrobiology; authigenic; clay

1. Introduction

Low-temperature mobility and redeposition of gold are well-established phenomena in the near-surface geological environment, and this gold mobility is commonly mediated by geomicrobiological processes [1–8]. In particular, bacteria have been shown experimentally to facilitate gold redeposition from encapsulating sulfide minerals, yielding crystalline and amorphous gold deposits at the nanometre scale [4–6,9–11]. Similar processes have been inferred for nanoparticulate and microparticulate crystalline and amorphous gold deposits in the natural environment in a range of geological settings [4–6,12,13].

Despite the well-established experimental and observational basis for geomicrobiological mediation of gold mobility, the details of the geochemical environments in which these processes occur are less well understood. This gap in knowledge arises because geomicrobiological agents and processes are ephemeral, and subject to overprinting by later events during the geological evolution of a host environment. Recent identification of the products and time scales of bacterially-mediated gold mobilisation in an active river [13] have helped to fill this knowledge gap for moist subtropical environments. In this study, we provide some geochemical and mineralogical constraints on geomicrobiological processes of gold mobility in a semiarid environment, where strong evaporative processes have been common.

This study provides observations on geochemistry and mineralogy of groundwater processes within Pleistocene fluvial sediments and immediately underlying basement rocks, and relates these observations to associated gold mobility and redeposition. These processes have occurred, and are still occurring, in an active tectonic environment, where uplift and erosion have caused physical recycling of placer gold to younger sediments, followed by renewed gold mobility involving both inorganic and biologically-mediated chemical processes. Evaporation has locally enhanced solution concentrations so that secondary minerals have formed with some of the new gold, providing some useful insights into the water geochemistry that accompanied gold mobility.

2. General Setting

A well-defined rain shadow zone has developed to the east of the mountains that form the backbone of the South Island of New Zealand (Figure 1a). This rain shadow results in semiarid climatic conditions with precipitation as low as 300 mm/year in inland areas, and the rain shadow effect has been present since at least the Pliocene [14,15]. Part of the rain shadow zone includes an area of Otago Schist basement that hosts numerous orogenic gold deposits that formed in the Cretaceous, including the world-class Macraes deposit that is an active mine on a regional structure, the Hyde-Macraes Shear Zone (Figure 1a,b) [16]. This study focuses on placer gold deposits within and near the 500 mm/year precipitation contour (Figure 1a). The region has potential evaporation greater than precipitation, resulting in widespread evaporative mineral formation at and near the landsurface (Figure 1a) [17–19]. Some evaporative salt deposits have formed in this region from surface evaporation of marine aerosols that were deposited on impermeable substrates [15,18,20].

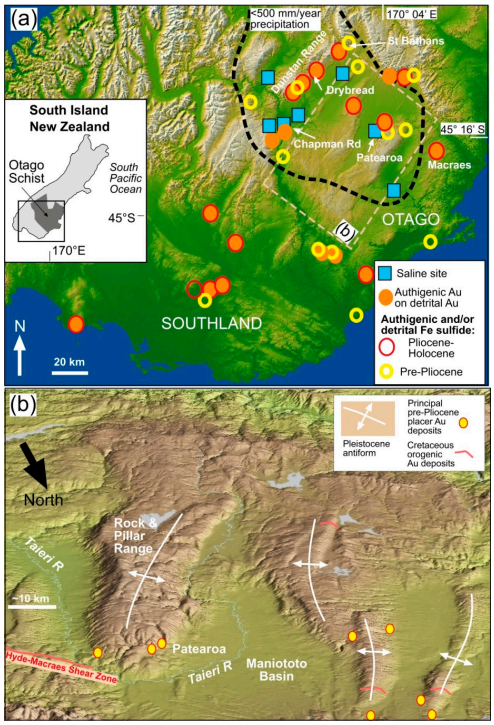

Figure 1. Location images for sites described in this study and their regional mineralogical and climatic contexts. (**a**) Digital elevation model map of southern New Zealand, showing part of the mountain chain to the west that causes a rain shadow, with the approximate boundary of the semiarid portion (black dashed contour). Localities referred to in the Table 1 and some other associated are indicated. Inset shows the extent of the Otago Schist belt, which hosts orogenic gold deposits that form the source for placers described herein; (**b**) Oblique digital elevation model (2 × vertical exaggeration) of the eastern part of the semiarid rain shadow (as indicated with dashed quadrilateral in **a**), showing tectonic topography and basement gold deposits.

Coupled with the rise of the main South Island mountain backbone, parts of the rain shadow area have been progressively uplifted since the Pliocene, but at relatively slow rates (<0.1–1 mm/year) [15,21]. This uplift has resulted in formation of a set of north to northeast trending antiformal mountain ranges, and these are separated by synformal basins in which little or no uplift has occurred (Figure 1a,b). The antiformal ranges have been rising for at least the past million years, and dominate the topography of the rain shadow area (Figure 1a,b) [15,21]. The ranges generally have smooth topography, with only minor stream incision. The smooth topography reflects exhumation during uplift of a low-relief regional unconformity surface that has been cut into the schist basement progressively since the Cretaceous [15,21,22].

A veneer of sediments, at times >300 m thick, accumulated on the regional unconformity between Cretaceous and Pliocene. The sedimentary veneer was fluvial at the base, with incursion of marine sediments in the middle Cenozoic, followed by regression and return of terrestrial conditions in the late Cenozoic as the region was uplifted. Groundwater incursion from sediments into the basement has caused extensive clay alteration, commonly accompanied by oxidation, of the basement rocks immediately beneath the unconformity [14,19]. This alteration zone, which is up to 100 m thick, developed progressively since the Cretaceous [14], and despite rapid erosion from the tops of antiformal ranges it is still preserved on the lower slopes of these ranges and beneath the synformal basins (Figure 2a) [15].

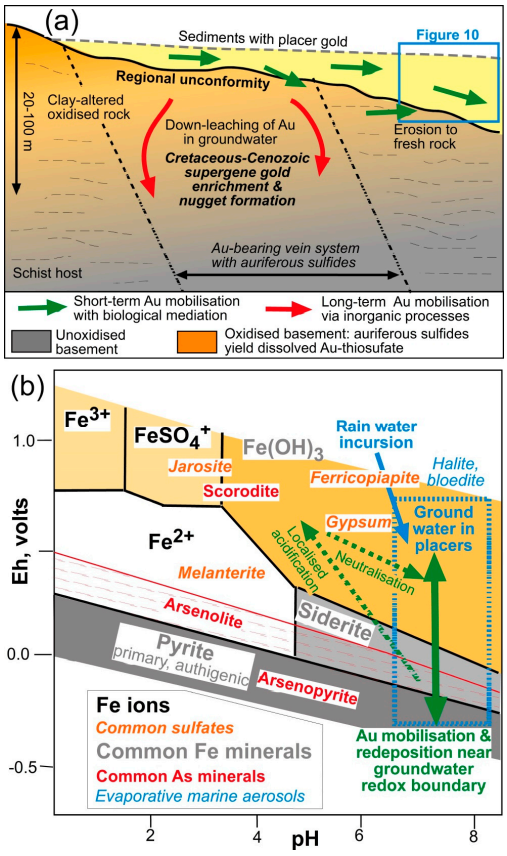

Figure 2. Summaries of principal geological, geochemical, and mineralogical features of near-surface gold mobility and redeposition within the Otago rain shadow. (**a**) Sketch cross section through the regional unconformity groundwater alteration zone in which long-term supergene gold enrichment has occurred to form nuggets since the Cretaceous. A sedimentary veneer has short-term gold mobility that is at least partially biologically mediated and is the focus of this study; (**b**) Sketch Eh-pH diagram, summarised from Geochemists Workbench modelling, showing the pH and redox relationships among minerals found within the placer gold sediments and basement, as outlined in this study.

Rise of the antiformal ranges has caused some erosion of basement schist and recycling of Cenozoic sediments, to form landslides and alluvial fans along the margins of the ranges and extending into the intervening basins (Figures 1b and 3a) [23,24]. Within the rain shadow area of this study, these alluvial fans are principally middle to late Pleistocene and Holocene in age. Early-formed fans have been uplifted and re-eroded into younger fans through the Pleistocene, and this process is still continuing as the area is tectonically active [15,21,22]. The sediments in the alluvial fans are typically poorly sorted gravels with angular or subrounded schist debris (Figure 3c). These deposits have been derived from short steeply incised streams on range margins during periodic rainstorms, with some similar matrix-supported debris flow material interlayered locally.

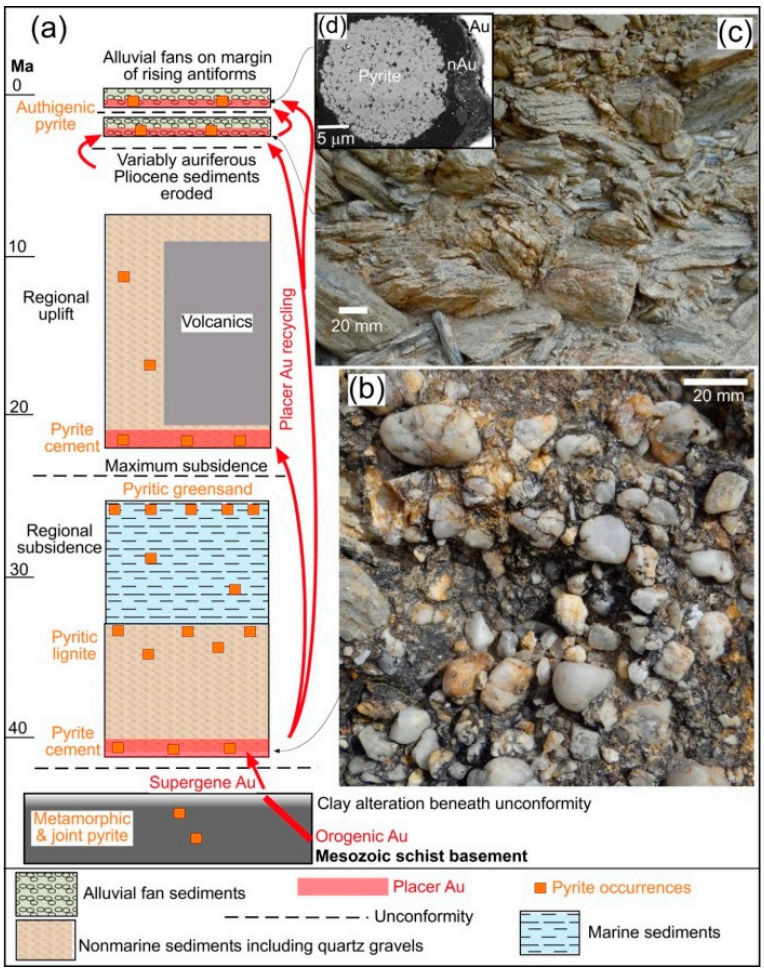

Figure 3. Stratigraphic setting for placer gold deposits in the eastern portion of the Otago rain shadow (Figure 1b). (**a**) Summary stratigraphic column, showing the principal rock types in the remnants of the sedimentary veneer, widespread distribution of authigenic pyrite, and typical placer gold recycling pathways; (**b**) Typical quartz pebble conglomerate, which is Eocene in this case, but recycled to Miocene farther inland; (**c**) Typical Pleistocene lithic conglomerate dominated by schist debris and cemented by clays and Fe oxyhydroxide, in outcrop above the water table; (**d**) scanning electron microscopy (SEM) image of a polished section of framboidal authigenic pyrite (left) coexisting with clay impregnated with nanoparticulate gold (nAu) and detrital gold (right).

3. Placer Gold

Most (>95%) primary hydrothermal gold in the Otago Schist goldfield is encapsulated in sulfide minerals, pyrite, and arsenopyrite, as micron scale particles [25–29]. These gold particles are too small to form significant placers during erosion. However, long-term alteration of the schist basement

beneath the regional unconformity has also affected the orogenic gold deposits, principally via oxidation of the sulfide minerals. Oxidation of associated sulfides has liberated the encapsulated gold, which was chemically mobilised by the groundwater and carried towards the base of the alteration zone (Figure 2a) [19,25]. The gold accumulated within supergene enrichment zones as coarser grained particles, including some centimetre scale nuggets [19,25].

Erosion of the supergene zone in the altered basement has been the principal contributor of gold particles to placer deposits that have formed progressively since the Cretaceous in various fluvial deposits in the sedimentary veneer (Figures 2a and 3a) [28,30,31]. On-going uplift and erosion, especially in the late Cenozoic, has caused recycling of detrital gold from early-formed placers into younger placers (Figure 3a). Paleoplacers locally remain as uneroded remnants on the flanks of the antiformal ranges in the rain shadow area, and some of these are as old as Eocene (Figure 1a,b and Figure 3a,b) [32]. Eocene and Miocene placers are dominated by recycled quartz pebbles (Figure 3b), whereas younger placers are dominated by lithic material derived directly from schist basement (Figure 3c).

4. Rationale and Methods

This paper involves a compilation of observations on gold and related geochemical and mineralogical data from a range of sites that have recently been described in more detail elsewhere [27,32–34]. These previous descriptions, and other related papers [19,25] have focused on the nature, formation, and proximal erosion of large (centimetre scale) gold nuggets from supergene gold enrichment zones that formed during long-term (since Cretaceous) groundwater alteration (Figure 2a). Smaller scale overgrowths, of biologically-mediated origin, on the rims of these larger particles were mentioned only casually in these earlier works.

In this paper, we focus on the fine grained overgrowths and compile data from a range of different settings where specific mineralogical and geochemical data are available. Late Pleistocene placers are the principal topic of this study as their detrital gold has been the recipient of geomicrobiologically-mediated overgrowths of new gold from groundwater systems (Figure 2a) that are still essentially the same as when the placers formed. We focus on five different geological settings from the semiarid rain shadow zone at which we have mineralogical and geochemical constraints on the environments in which the overgrowths formed, principally in the Late Pleistocene and/or Holocene (Table 1 and Figure 1a).

Mineral identifications were carried out with standard light microscopy, X-ray diffraction, and scanning electron microscopy (SEM) with energy dispersive analytical attachment. Equipment and operating conditions are described in more detail in the above-cited references. Identification of specific Fe sulfate minerals at the micron scale was not possible other than confirmation of the general elemental compositions with SEM. These Fe sulfate minerals vary widely with degree of hydration, which can also change after sampling and preparation for SEM examination. Groundwater analyses were obtained from a range of commercial laboratories, as outlined in various references cited herein.

Table 1. Summary of the key geological and mineralogical features of gold-bearing localities described in the text, with principal biologically-mediated authigenic gold textures.

Locality	Chapman Rd	St Bathans	Macraes	Patearoa	Drybread
Placer age	Miocene-Holocene	Miocene	Late Pleistocene-Holocene	Late Pleistocene-Holocene	Late Pleistocene
Host	Schist & quartz pebble debris, alluvial fan	Quartz pebble conglomerate	Schist debris, alluvial fan	Schist & quartz pebble debris, alluvial fan	Schist & quartz pebble debris, alluvial fan
Geological setting	Base of active fault scarp, on regional unconformity	Active fault zone, tilted strata on regional unconformity	Base of active fault scarp in shallow Pleistocene basin	Flanks of active antiformal range	Flanks of active antiformal range
Au particles	Supergene nuggets (cm)	Detrital flakes (<1 mm)	Supergene nuggets (mm)	Detrital, angular (<1 mm)	Detrital flakes (<1 mm)
Au transport	Proximal (<100 m)	Distal (>10 km)	Proximal (<100 m)	Proximal (<5 km)	Distal (? km)
Au recycling	Minor	Several generations	Nil	Several generations	Several generations
Sulfide relationships	Partially oxidised metamorphic & Miocene authigenic pyrite	Partially oxidised metamorphic & Miocene authigenic pyrite	Partially oxidised hydrothermal & detrital pyrite & arsenopyrite; authigenic pyrite below redox boundary	Partially oxidised metamorphic pyrite; authigenic pyrite below redox boundary	Partially oxidised metamorphic pyrite; authigenic pyrite below redox boundary
Groundwater	Ephemeral, abundant evaporative salts (mainly marine aerosols)	Partially saturated; evaporative sulfates	Partially saturated; evaporative sulfates, arsenolite & arsenates	Partially saturated; evaporative sulfates	Partially saturated; evaporative sulfates
pH	5.6–8.0	7.0–7.8	6.8–8.2	7.3–8.0	7.3–8.6
Au particle authigenic overgrowths	Abundant; vermiform, crystalline	Abundant; plates, vermiform	Abundant; vermiform	Abundant; plates vermiform, crystalline	Common, vermiform
Authigenic Au-mineral intergrowths	Kaolinite; nano & micro-particulate Au	Kaolinite; nano & micro-particulate Au	Fe sulfate; nano & micro-particulate Au	Undifferentiated clays; nano & micro-particulate Au	Undifferentiated clays; nano & micro-particulate Au
References	[18,19]	[33]	[25,27]	[32]	[24]
Illustrations	Figure 5	Figure 6	Figure 7	Figures 3 and 8	Figure 9

5. Authigenic Minerals

5.1. Clay Minerals

Groundwater-driven alteration of silicate minerals has caused formation of authigenic clay minerals within basement and sediments [14], similar to that which has occurred near to regional unconformities elsewhere in the world [35,36]. There are two principal alteration pathways involving phyllosilicates above and below the sulfide-sulfate redox boundary: (i) alteration of muscovite to illite and ultimately to kaolinite; and alteration of Fe-bearing phyllosilicates (principally chlorite) to smectite-vermiculite and ultimately to kaolinite [14,30]. Alteration of albite to kaolinite occurred under oxidising conditions as well. These processes advanced to kaolinite beneath the regional unconformity, and within the basal sediments, as a result of long-term alteration since the Cretaceous, and some rocks have been completely kaolinitised. Authigenic clay formation via these processes has been only incipient in Pleistocene sediments, but fine-grained (micron scale) authigenic illitic and smectite-vermiculite clays are widespread in the matrix of even young schist-rich sediments, causing localised cementation and lithification of the sediments (e.g., Figure 3c) [14,34].

5.2. Pyrite in Near-Surface Environments

Metamorphic pyrite is a common component of the schist basement outside of unoxidised orogenic gold deposits, although this pyrite forms only ~1% of the rocks. Groundwater remobilisation of metamorphic pyrite has been widespread within the schist basement, resulting in formation of authigenic pyrite on schist joint surfaces and in parts of the clay alteration zone (Figure 3a) [14,37]. Formation of this authigenic pyrite has occurred below the sulfate-sulfide redox boundary, which has fluctuated widely throughout the long-term evolution of the regional unconformity alteration zone (Figure 2a,b) [37].

Authigenic pyrite deposited by seawater in marine sediments and groundwater in nonmarine sediments is distributed throughout the sedimentary veneer, in sediments of all ages (Figure 3a). This pyrite occurs in pore spaces as framboids (Figure 3d), clast coatings, and locally as a pervasive cement in the sediments [17,37]. Sulfur to form this pyrite has been derived from the underlying basement, directly from seawater, and from downward percolation of groundwater containing marine aerosol sulfate [17,37].

Rapid erosion and redeposition of pyrite-bearing rocks has resulted in preservation of detrital pyrite in many of the fluvial sediments, especially the fan deposits on the margins of rising basement ranges [23,27,37]. This detrital pyrite includes liberated particles that are typically sand-sized, but is dominated by remnant metamorphic and authigenic pyrite attached to, and within, larger silicate clasts. Oxidation of the metamorphic, authigenic, and detrital pyrite and other associated Fe-bearing minerals in basement and sediments has yielded abundant Fe oxyhydroxide (typically amorphous or two-line ferrihydrite, $Fe^{III}[OH]_3$) which has generally replaced the pyrite pseudomorphously [19,30,31]. Hence, Fe oxyhydroxide joint coatings are widespread in the oxidised zone beneath the regional unconformity, and Fe oxyhydroxide staining and cements are common above the groundwater sulfide-sulfate redox boundary in the sedimentary veneer (Figures 2a,b and 3c).

5.3. Sulfate Minerals

The widespread and diverse occurrences of pyrite within the basement and overlying sediments ensures that near-surface oxidation of the rocks results in formation of sulfate minerals. The most common sulfate minerals (Figure 2b) include gypsum ($CaSO_4 \cdot 2H_2O$), melanterite ($Fe^{II}SO_4 \cdot 7H_2O$), ferricopiapite ($Fe^{III}{}_{2/3}Fe^{III}{}_4[SO_4]_6[OH]_2 \cdot 20H_2O$), jarosite ($KFe^{III}{}_3[SO_4]_2[OH]_6$), and bloedite ($Na_2Mg[SO_4]_2 \cdot 4H_2O$). These minerals contribute to evaporative coatings on outcrop surfaces and joints, and cements of surficial sediments, especially beneath overhangs that are protected from occasional rain events [15,17–19]. Most such coatings also include evaporative calcite and/or halite

(Figures 2b and 5a). Sulfate minerals also locally coat sulfide minerals at the micron scale where the sulfides have undergone partial oxidation [27,29].

5.4. Arsenic Minerals

Arsenopyrite is a common mineral, forming up to 5% of the rock in primary hydrothermal gold deposits of the schist basement. Oxidation of the arsenopyrite beneath the regional unconformity has yielded widespread scorodite ($Fe^{III}As^{V}O_4 \cdot 2H_2O$) as direct pseudomorphous replacement of arsenopyrite crystals and as evaporative coatings on joint surfaces (Figure 2b) [25,27]. Incipient oxidative alteration of arsenopyrite can also result in minor amounts (micron scale) of arsenolite ($As^{III}_2O_3$) as an intermediate oxidation product (Figure 2b), typically on the surface of arsenopyrite particles [27,29]. For example, detrital arsenopyrite derived from rapid erosion of mineralised rocks with immediate sedimentary burial below the water table also has minor amounts of arsenolite as an intermediate oxidation product on particle surfaces [27,29].

6. Groundwater Compositions

Groundwater in Pleistocene basins that contain abundant schist debris typically has pH between 7 and 8, with some localised trends towards lower pH (near to pH 6; Figure 4) [19]. This ambient high pH is a result of water-rock interaction with schist debris that contains abundant (typically at least 1–2%) metamorphic calcite [19,25,38]. Incursion of rainwater with pH near 6 contributes to the localised lower pH (Figure 2b), but rapid reaction with the calcite on a time scales of weeks to years [38] ensured that pH remained high. This high pH is a widespread feature of almost all waters in schist basement and schist-bearing overlying sediments including Pleistocene sediments that contain placer gold (Figure 4). The calcite dissolution and neutralisation reactions in the basement and sediments results in high alkalinity (typically 200–800 mg/L as HCO_3^-) in these waters [19,38].

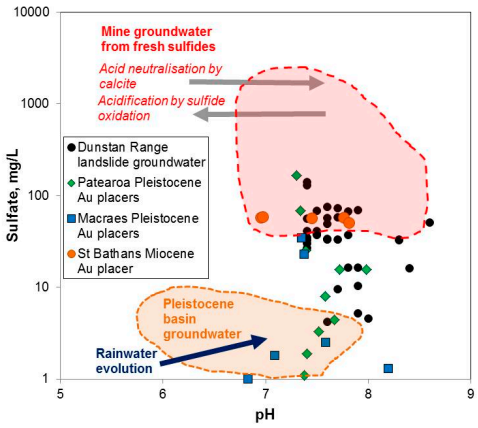

Figure 4. Groundwater pH and dissolved sulfate concentrations for gold placer deposits (Table 1) and associated sediments, landslides, and basement rocks.

Typical basin groundwaters have low dissolved sulfate concentrations (<10 mg/L; Figure 4). This dissolved sulfate is derived from a combination of incursion of marine aerosols in rain and interaction with pyrite-bearing rocks [17,37–39]. Locally, extensive interaction between oxidising groundwater and the widespread pyrite causes elevated dissolved sulfate concentrations in the groundwater, with concentrations reaching ~100 mg/L where groundwaters percolate slowly through relatively impermeable lithic debris such as poorly sorted alluvial fan sediments and landslides (Figures 3c and 4) [19,34]. Neutralised mine waters can have even higher dissolved sulfate concentrations (Figure 4). These high concentrations of dissolved sulfate are further elevated by evaporation in the semiarid environment, resulting in precipitation of sulfate minerals as well as some of the other evaporative minerals (Figure 2b).

7. Biogenic Gold Textures

The gold overgrowth textures observed within the rain shadow region are similar at numerous sites in southern New Zealand (Figure 1a) [4,6,12,19,32,39]. The textures are dominated by irregular micron-scale vermiform gold shapes that have precipitated on the exterior of detrital gold particles. At least some of the vermiform textures have been likened to accumulations of colloidal gold rather than products of direct chemical precipitation, although no specific evidence of a colloidal intermediate has yet been found [12]. Some of the vermiform masses locally merge to form gold plates. In addition, some micron-scale crystalline gold is associated with the vermiform masses. Triangular and hexagonal crystal plates are the most common crystalline form, and dodecahedral gold crystals also occur locally. These features have formed in placers of various ages, from Eocene to Holocene and have then been deformed and obscured by recycling-related transport to reform in their new environment in younger placers [19,32,34]. In the following site descriptions, we focus on the youngest stage of detrital gold deposition in which the delicate overgrowth textures are still best preserved.

7.1. Miocene Placer Gold

At the Chapman Road saline site (Table 1; Figures 1a and 5a), large gold nuggets have been derived from the exposed long-term supergene enrichment zone in mineralised rocks underlying the partially eroded regional unconformity. The nuggets are made up of coarse (up to 1 mm) internal crystalline grains, and some external surfaces are defined by large (mm-scale) crystal facets (Figure 5b). These nuggets have been transported only metres to hundreds of metres since the adjacent fault zone became active in the Miocene and the gold was incorporated into Miocene quartz pebble conglomerate. Subsequent fault-related uplift has caused recycling of the gold into younger alluvial fans, the last of which formed in latest Pleistocene. This proximal transport has caused some rounding of the nuggets, especially on protruding crystal corners. Since the last stage of transport, abundant gold overgrowths have formed on some exterior surfaces (Figure 5c–e). Micron-scale vermiform gold adheres to nugget surfaces and is also intergrown with authigenic kaolinite in cavities in the nugget surfaces (Figure 5c–e). Dusty nanoparticulate gold also occurs dispersed through the authigenic kaolinite (Figure 5c).

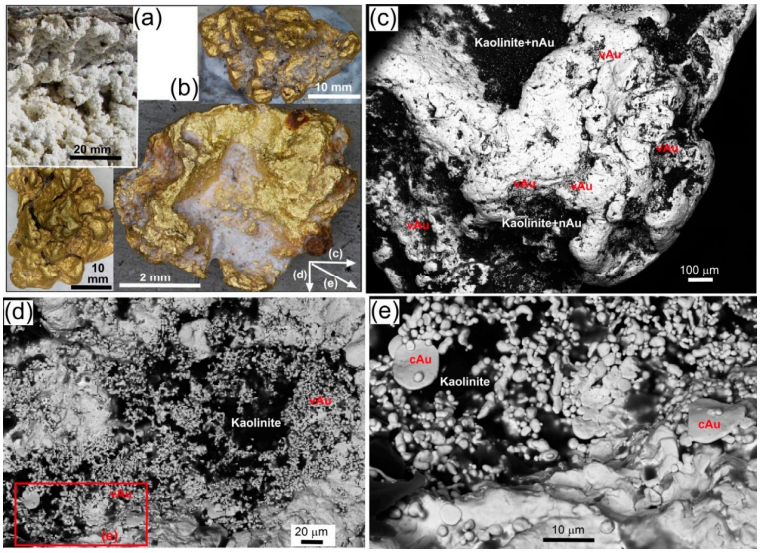

Figure 5. Mineralogical features of the Chapman Road saline site (Table 1; Figure 1a). (**a**) Evaporative encrustations on outcrop, dominated by halite, bloedite, calcite, and gypsum; (**b**) Three large gold nuggets from Late Pleistocene fan gravels resting on the regional unconformity; (**c**) SEM backscatter electron image of a portion of the indicated nugget in a, with abundant vermiform authigenic gold (vAu); (**d**,**e**) Closer views of surface of nugget in (**c**), with vermiform and crystalline (cAu) authigenic gold.

More distal Miocene detrital gold, without subsequent recycling, occurs in structurally-controlled remnants of quartz pebble conglomerates near St Bathans (Table 1; Figure 1a). Rounded and flattened gold particles contain detrital and authigenic kaolinite in cavities (Figure 6a–c). Relict supergene crystalline gold textures are locally preserved where portions of the detrital cores are exposed (Figure 6c). However, large parts of the detrital surfaces are covered at the micron scale with gold plate overgrowths, and some of these plates protrude with delicate textures into open cavities (Figure 6b–d). In addition, nanoparticulate authigenic gold is commonly dispersed through the surficial kaolinite (Figure 6b,d).

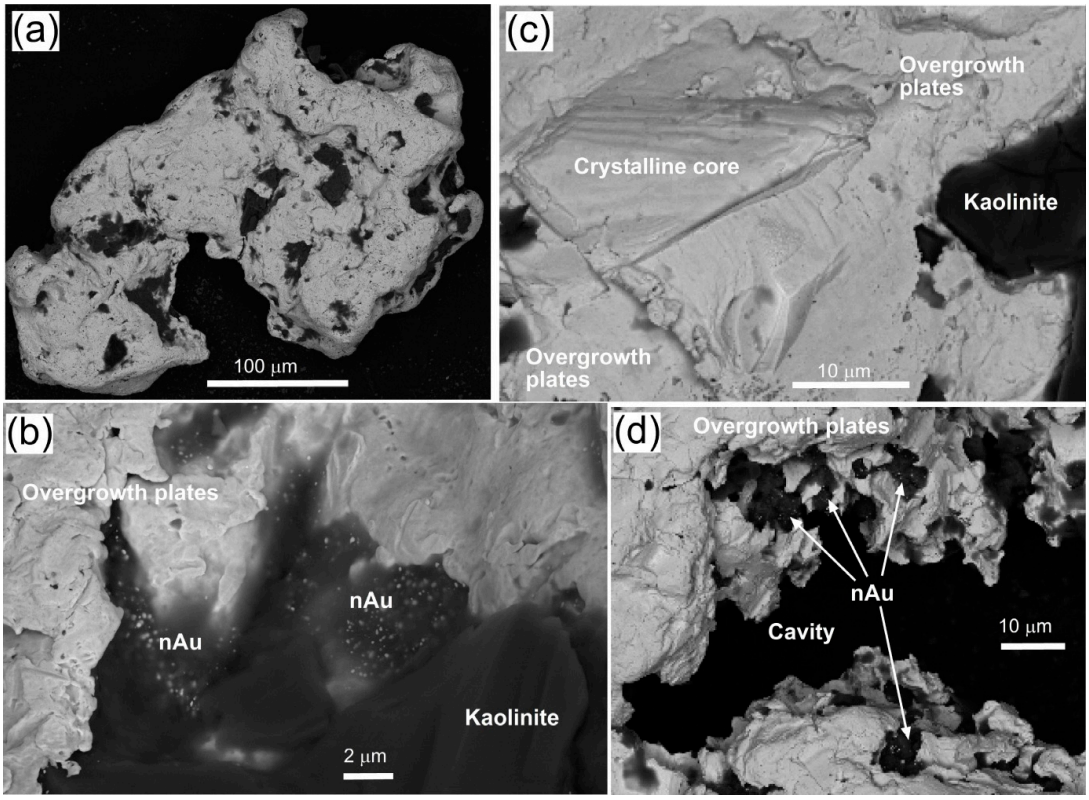

Figure 6. SEM backscatter electron images of surface features of detrital gold from Miocene quartz pebble conglomerate from the St Bathans area. (**a**,**b**) Gold from Pennyweight excavation, with overgrowth plates and nanoparticulate gold (nAu) intergrown with kaolinite; (**c**,**d**) Gold from Blue Lake excavation showing overgrowth plates on a crystalline core, with delicate overgrowth plates extending into an open cavity.

7.2. Late Pleistocene Gold Placers

Detrital gold derived by erosion of the partially eroded long-term supergene enrichment zone at Macraes (Table 1; Figure 1a) has accumulated in thin (<10 m) Late Pleistocene-early Holocene alluvial fan sediments immediately adjacent to the mineralised basement. The sediments, 12–20 ka in age, contain abundant detrital pyrite and arsenopyrite derived from the mineralised basement, and organic-rich portions of the sediments also contain authigenic framboidal pyrite. The sediments have a fluctuating water table as the ephemeral surface drainage streams dry up seasonally, and hence the depth of the sulfide-sulfate redox boundary (Figure 2b) has fluctuated as well. Evaporative concentration of groundwaters in the sediments has caused localised precipitation of sulfate minerals along with Fe oxyhydroxide as sulfide minerals have become oxidised. The proximal detrital gold particles are generally angular or subrounded, and many have intergrown Fe oxyhydroxide and Fe sulfate (Figure 7a). Authigenic gold has overgrown the detrital gold particles, and is commonly

intergrown with the coating iron oxyhydroxide and/or Fe sulfate (Figure 7a–d). Authigenic gold locally fills desiccation cracks in amorphous evaporative Fe sulfate, and is commonly intergrown with crystalline Fe sulfate (Figure 7b,c). The authigenic gold overgrowths occur at nanometre and micron scales (Figure 7b–d).

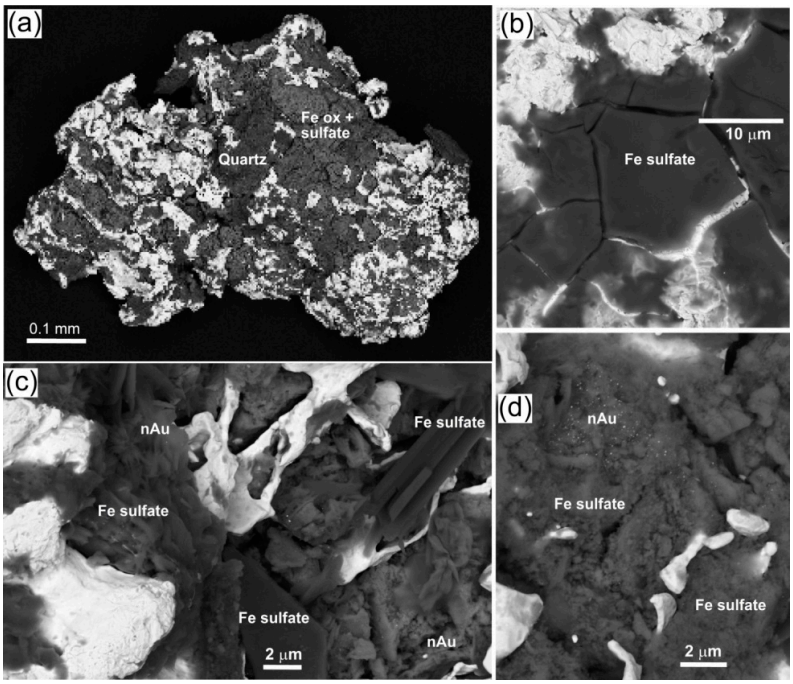

Figure 7. SEM backscatter electron images of surface features of proximal detrital gold in Late Pleistocene-Holocene sediments derived from the Macraes orogenic deposit. (**a**–**d**) Authigenic gold is intergrown with evaporative Fe oxyhydroxide and Fe sulfate deposits at a range of scales including nanoparticulate gold (nAu).

Detrital gold in Pleistocene alluvial fans near Patearoa (Table 1; Figures 1a,b and 3) was derived from the Macraes mineralised zone or a related structure, and was recycled through Eocene quartz pebble conglomerate (Figure 3b). However, the gold is relatively proximal to its ultimate source, and particles are angular to subrounded in shape with detrital and authigenic clays in cavities (Figure 8a). The interior of the particles have retained original coarse grained structure, although the rims of the particles have finer grain size as a result of transport-related deformation which drove minor recrystallisation (Figure 8b). Authigenic gold overgrowths have formed on the outside of the recrystallised rims after deposition in the Late Pleistocene sedimentary deposits, the youngest of which may be early Holocene. Vermiform and crystalline authigenic gold adheres to the gold particles and is intergrown with clay on particle surfaces (Figure 8c–f).

The latest Pleistocene Drybread alluvial fan emanates from the rising Dunstan Range antiform (Table 1; Figure 1a), and the fan debris is made up of a combination of freshly eroded schist basement and recycled schist clasts and quartz pebbles from earlier-formed fan deposits [23]. Portions of Pleistocene fans that are buried below the water table are partially cemented by authigenic pyrite and Fe^{II}-bearing authigenic clays, locally intergrown with microparticulate and nanoparticulate gold. Surficial deposits are variably cemented by undifferentiated authigenic clays and Fe oxyhydroxide. Much of the detrital gold has rounded and abraded surfaces, and most particles have been flattened to form flakes (Figure 9a,b) as a result of transport-related deformation. Cavities in the gold particle surfaces are filled with authigenic and detrital clays, and most of this clay has intergrown nanoparticulate and microparticulate authigenic gold (Figure 9c–e). Authigenic vermiform gold and gold plates locally coat gold particle surfaces and span clay-filled cavities (Figure 9c–e).

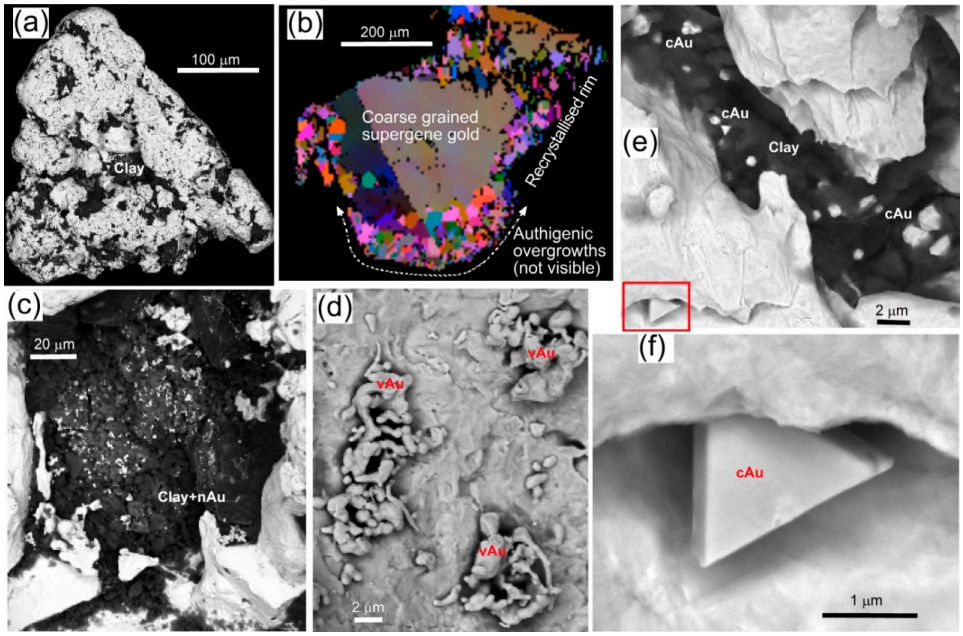

Figure 8. SEM images of detrital gold from Late Pleistocene gravels of the Patearoa area (Figures 1a,b and 3a,c). (**a**) Electron backscatter image of exterior surface of a detrital particle; (**b**) Electron backscatter diffraction image (Euler colours) of a polished section etched with *aqua regia*, showing the coarse grained internal structure derived from supergene source, and a rim of finer grained gold recrystallised after transport-induced deformation. Authigenic overgrowths (not visible in (**b**); as in (**c**–**f**) coat the rims; (**c**–**f**) Electron backscatter images of authigenic gold overgrowth textures (nAu = nanoparticulate; vAu = vermiform; cAu = crystalline).

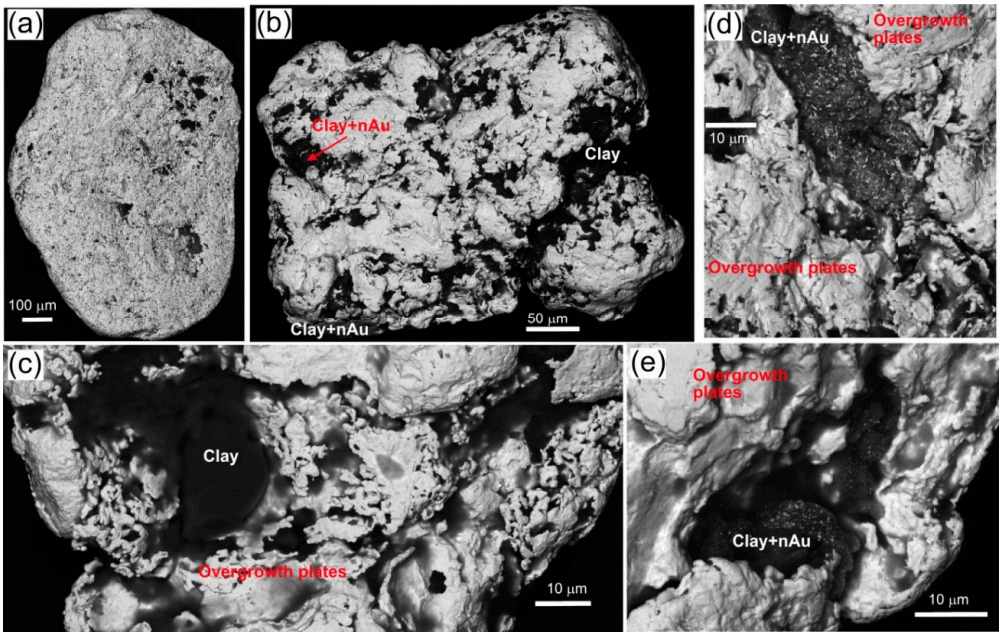

Figure 9. SEM backscatter electron images of surface features of detrital gold in Late Pleistocene sediments in the Drybread area (Figure 1a). (**a**,**b**) Typical transported detrital particles; (**c**–**e**) Authigenic gold has overgrown the detrital particles as plates and vermiform masses, and is commonly intergrown with authigenic clays (nanoparticulate gold = nAu).

8. Discussion

8.1. Geochemical Environment of Gold Mobilisation

Mineralogical observations on the gold placers suggest that the geochemical environment has been dominated by authigenic sulfur minerals at neutral to alkaline pH (Table 1; Figure 2b). The particular sulfur minerals that have formed in these placers depended on the redox state of the immediate environments: sulfides, mainly pyrite, dominate below the water table, whereas sulfates dominate above the water table. This distinction is not clear-cut as high evaporation associated with the semiarid climate has caused the position of the water table to fluctuate, and tectonic uplift has also affected the position of this redox boundary over time. The general spatial geometry of this dynamic environment is summarised in Figure 10a.

Groundwater-driven oxidation of sulfides within the sediments and underlying basement can generate sulfuric acid, but on a scale of metres to hundreds of metres, any sulfuric acid generated by pyrite oxidation near the fluctuating redox boundary is rapidly neutralised by calcite within the sediments and basement (Figures 2b and 4). Hence, high pH is typically maintained in both surface and ground waters [38,40,41]. Even sulfide-rich rocks exposed by mining have had acid immediately neutralised on a mine scale (Figure 4) [38]. Experimental work on oxidation of sulfide bearing rocks in general shows localised acidification at the centimetre scale, but any such acid generation has been neutralised at larger scales in the placers of this study (Table 1; Figures 2b and 4) [29,38,42].

Evaporation of marine aerosols has caused increased concentrations of dissolved components, especially the dominant Na and Cl ions, leading locally to halite deposition on the surface of some Otago placer sediments (Figure 5a) [18,20]. However, even these salt-rich deposits contain sulfate minerals, principally bloedite and gypsum, and the pH of these salt encrustations is typically alkaline (Table 1) [18,20].

8.2. Biologically-Mediated Gold Solubility

Experimental studies with bacteria in gold-bearing environments suggest that gold mobilisation and deposition is a byproduct of bacterial life-processes rather than a direct result of bacterial corrosion of gold [4,9–11]. In particular, generation of thiosulfate ions, as metastable intermediates in the oxidation of sulfide minerals to ultimately yield dissolved sulfate ions, is an important component of bacterially-mediated gold dissolution [11]. Gold-thiosulfate complexation is distinctly more significant for gold dissolution than Au–Cl or Au–OH complexes under oxidising and circumneutral conditions that have prevailed in most of the Otago placer deposits (Figure 10b) [43,44].

Thiosulfate ions can be generated via a range of pathways in this sulfide oxidation process, and bacterial effects are especially effective where localised acidification has occurred [11,45,46]. Once thiosulfate ions have been generated, gold can dissolve via a net reaction summarised as Equation (1) (Figure 10b) [46–48]:

$$4Au + 8S_2O_3^{2-} + O_2 + 2H_2O \Rightarrow 4[Au(S_2O_3)_2]^{3-} + 4OH^- \quad (1)$$

Gold dissolution via thiosulfate complexation is most rapid (hours to days) when catalysed by divalent metal ions [46,49,50], but can also occur on time scales of weeks to months without such catalysis, especially at high pH (Figure 10b) [47]. The ephemeral nature of thiosulfate ions in the geological environment ensures that, once dissolved, the gold will ultimately be redeposited (Figure 10b). Variations in redox state and/or pH of groundwater with dissolved Au-thiosulfate complexes can readily cause gold deposition (Figure 10b) [19,47,51]. Likewise, evaporative concentration of groundwater in the surficial zone of Otago placers may have contributed to gold deposition (e.g., Figure 7b).

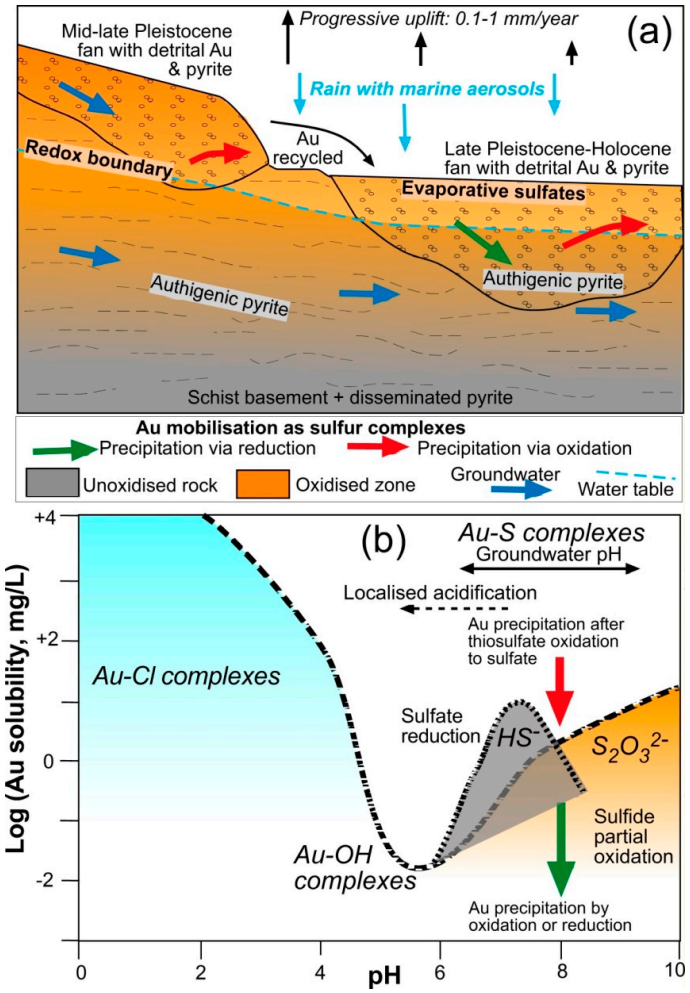

Figure 10. Summary diagrams highlighting the key features of biologically-mediated authigenic gold mobility in Late Pleistocene alluvial fans on the flanks of tectonically active antiformal ranges (Figure 1a,b). (**a**) Sketch cross section through a portion of the sedimentary veneer as indicated in Figure 2a, showing the fluctuating redox boundary that controls oxidised and reduced gold mobilisation processes (see text); (**b**) Variations in gold solubility with pH in near-surface groundwater, for differing redox conditions as in a (modified from [19], from references quoted in text).

Gold dissolution in circumneutral pH groundwater can also occur via complexation with reduced sulfide species, which are stable below the sulfide-sulfate redox boundary (Figures 2b and 10b) [8,47]. Bacterially-mediated reduction of sulfate to sulfide species can occur via a net reaction such as Equation (2) [52], with dissolved organic matter derived from coal and/or soil in the shallow sedimentary environment:

$$2CH_2O + SO_4^{2-} => 2HCO_3^- + H_2S \quad (2)$$

The H_2S dissociates to HS^- ions under more alkaline conditions, and gold dissolution followed by reprecipitation of that gold is sensitive to pH and redox state (Figures 3d and 10b) [8,47]. Hence, gold mobilisation and redeposition has occurred both above and below the sulfide-sulfate redox boundary (Figures 2b and 10a,b), and has been controlled by minor changes in pH and Eh while being enhanced by both sulfur-oxidising and sulfur-reducing bacterial activity that generated the requisite sulfur ligands.

Within the context of the above reactions, gold mobilisation and redeposition processes have been enhanced by the arid climate as a result of two principal effects: (a) fluctuations in the water table; and

(b) localised evaporative concentration of groundwater compositions. The variations in position of the water table have caused changes in aqueous redox potential, leading to fluctuations of stability of the dominant sulfur species near the sulfide/sulfate redox boundary, especially affecting the stability of primary and authigenic pyrite (Figures 3a and 10a). Consequently, thiosulfate and bisulfide ligands for gold solubility have been periodically mobilised near to the fluctuating water table, facilitated by bacteria. Concentrations of these ligands, and associated dissolved gold (Figure 10b), were affected by both evaporative concentration and redox fluctuations.

9. Conclusions

Regional tectonic uplift since the Miocene has exposed paleoplacer gold deposits and orogenic gold deposits in the underlying basement in the Otago Schist belt of southern New Zealand. Rise of higher mountains to the west has caused a semiarid rain shadow zone to develop over the area. Erosion and sedimentary recycling during on-going uplift in this rain shadow has yielded gold-bearing Late Pleistocene to Holocene alluvial fans (Figure 10a) in which biologically-mediated gold mobility has occurred in groundwater. Resultant micron-scale authigenic gold overgrowths on detrital gold particles are widespread (Figures 5–9). The products of this short-term and small scale gold mobility are different from long-term supergene enrichment of gold in the basement that has been enhancing gold particle sizes via inorganic processes since the Cretaceous, with some centimetre scale nugget formation (Figure 2a).

Sediments of all ages since the Eocene that rest on the basement in the rain shadow area contain detrital and authigenic pyrite below a redox boundary that approximately coincides with the water table (Figure 10a). Oxidation of pyrite above this redox boundary yields elevated concentrations of dissolved thiosulfate and ultimately sulfate in groundwater. The abundant calcite in sediments and underlying basement inhibits all but localised (cm scale) acidification of the groundwater environment during this pyrite oxidation, and pH remains circumneutral to alkaline (Figure 10b). Strong evaporation in the semiarid climate caused further enhancement of water concentrations, resulting in precipitation of sulfate minerals, predominantly gypsum and Fe sulfates, in the near-surface environment (Figure 10a). Marine aerosols in rain have contributed additional dissolved components including some evaporative halite and bloedite. The position of the sulfide-sulfate redox boundary in the near-surface environment has varied over time because of on-going tectonic uplift and fluctuating groundwater levels in the semiarid climate (Figure 10a).

Gold has been mobilised chemically in this groundwater environment as Au-sulfur complexes, with the S-bearing ligands (HS^-, $S_2O_3^{2-}$) being derived from bacterially-mediated oxidation and reduction processes. Oxidation of pyrite has been the dominant process, and this yielded metastable thiosulfate ions that dissolved and then redeposited gold on the surfaces of detrital gold particles as a result of redox and pH variations (Figure 10b). In addition, bacterially-mediated reduction of dissolved sulfate below the water table yielded reduced sulfur species that also dissolved and redeposited gold as overgrowths (Figure 10b). Despite the localised high dissolved chloride concentrations in evaporitic environments, the high pH precluded significant involvement of Au–Cl complexes in gold mobility (Figure 10b).

Acknowledgments: This research was supported financially by the Marsden Fund administered by Royal Society of New Zealand, with additional support from NZ Ministry of Business Innovation and Employment, and University of Otago. Mark Hesson kindly provided access to his gold nugget collection. Discussions with Joanna Druzbicka, Donna Falconer, Shanna Law, Dave Prior, Frank Reith, Cathy Rufaut, Gordon Southam, and John Youngson helped with formulating various aspects of this work. Technical assistance was provided by Luke Easterbrook-Clarke and Brent Pooley. Scanning electron microscope images were captured with the able assistance of Kat Lilly at the Otago Centre for Electron Microscopy. Reviews by two anonymous referees improved the presentation of the ms.

Author Contributions: Gemma Kerr is a student at University of Otago, working under the supervision of Professor Dave Craw, and this research project has been developed collaboratively as part of the PhD programme. Gemma Kerr has conducted field work in the arid areas, especially around Patearoa, has obtained placer gold specimens from miners and exploration geologists, and has conducted extensive SEM examination of the resultant

material. Dave Craw has been responsible for providing regional context for this research and obtaining funding for long-term studies of gold in the Otago goldfield.

Conflicts of Interest: The authors declare no conflicts of interest.

References

1. Webster, J.G.; Mann, A.W. The influence of climate, geomorphology and primary geology on the supergene migration of Au and Ag. *J. Geochem. Explor.* **1984**, *22*, 21–42. [CrossRef]
2. Bowell, R.J. Supergene gold mineralogy at Ashanti, Ghana: Implications for the supergene behaviour of gold. *Mineral. Mag.* **1992**, *56*, 545–560. [CrossRef]
3. Bowell, R.J.; Foster, R.P.; Gize, A.P. The mobility of gold in tropical rain forest soils. *Econ. Geol.* **1993**, *88*, 999–1016. [CrossRef]
4. Reith, F.; Lengke, M.F.; Falconer, D.; Craw, D.; Southam, G. The geomicrobiology of Au: International Society for Microbial Ecology. *ISME J.* **2007**, *1*, 567–584. [CrossRef] [PubMed]
5. Reith, F.; Fairbrother, L.; Nolze, G.; Wilhelmi, O.; Clode, P.L.; Gregg, A.; Parsons, J.E.; Wakelin, S.A.; Pring, A.; Hough, R.; et al. Nanoparticle factories: Biofilms hold the key to Au dispersion and nugget formation. *Geology* **2010**, *38*, 843–846. [CrossRef]
6. Reith, F.; Stewart, L.; Wakelin, S.A. Supergene gold transformation: Secondary and nanoparticulate gold from southern New Zealand. *Chem. Geol.* **2012**, *320*, 32–45. [CrossRef]
7. Lintern, M.; Anand, R.; Ryan, C.; Paterson, D. Natural gold particles in *Eucalyptus* leaves and their relevance to exploration for buried gold deposits. *Nat. Commun.* **2013**, *4*, 2274. [CrossRef] [PubMed]
8. Heinrich, C.J. Witwatersrand gold deposits formed by volcanic rain, anoxic rivers and Archaean life. *Nat. Geosci.* **2015**, *8*, 206–209. [CrossRef]
9. Lengke, M.; Southam, G. The deposition of elemental gold from gold (I) thiosulfate complexes mediated by sulfate-reducing bacterial conditions. *Econ. Geol.* **2007**, *102*, 109–126. [CrossRef]
10. Johnston, C.W.; Wyatt, M.A.; Li, X.; Ibrahim, A.; Shuster, J.; Southam, G.; Magarvey, N. Gold biomineralization by a metallophore from a gold-associated microbe. *Nat. Chem. Biol.* **2013**, *9*, 241–243. [CrossRef] [PubMed]
11. Shuster, J.; Lengke, M.; Marquez-Zavalia, M.F.; Southam, G. Floating gold grains and nanophase particles produced from the biogeochemical weathering of a gold-bearing ore. *Econ. Geol.* **2016**, *111*, 1485–1494. [CrossRef]
12. Falconer, D.M.; Craw, D. Supergene gold mobility: A textural and geochemical study from gold placers in southern New Zealand. In *Supergene Environments, Processes and Products*; Special Publications of the Society of Economic Geologists; Titley, S.R., Ed.; Society of Economic Geologists: Littleton, CO, USA, 2009; Volume 14, pp. 77–93.
13. Shuster, J.; Reith, F.; Cornelis, G.; Parsons, J.E.; Parson, J.M.; Southam, G. Secondary gold structures: Relics of past biogeochemical transformations and implications for colloidal gold dispersion in subtropical environments. *Chem. Geol.* **2017**, *450*, 154–164. [CrossRef]
14. Chamberlain, C.P.; Poage, M.A.; Craw, D.; Reynolds, R.C. Topographic development of the Southern Alps recorded by the isotopic composition of authigenic clay minerals, South Island, New Zealand. *Chem. Geol.* **1999**, *155*, 279–294. [CrossRef]
15. Craw, D.; Druzbicka, J.; Rufaut, C.; Waters, J. Geological controls on paleo-environmental change in a tectonic rain shadow, southern New Zealand. *Palaeogeog. Palaeoclim. Palaeoecol.* **2013**, *370*, 103–116. [CrossRef]
16. Mortensen, J.K.; Craw, D.; MacKenzie, D.J.; Gabites, J.E.; Ullrich, T. Age and origin of orogenic gold mineralisation in the Otago Schist belt, South Island, New Zealand: Constraints from lead isotope and $^{40}Ar/^{39}Ar$ dating studies. *Econ. Geol.* **2010**, *105*, 777–793. [CrossRef]
17. Youngson, J.H. Sulphur mobility and sulphur mineral precipitation during early Miocene-Recent uplift and sedimentation in Central Otago, New Zealand. *N. Z. J. Geol. Geophys.* **1995**, *38*, 407–417. [CrossRef]
18. Druzbicka, J.; Rufaut, C.; Craw, D. Evaporative mine water controls on natural revegetation of placer gold mines, southern New Zealand. *Mine Water Environ.* **2015**, *34*, 375–387. [CrossRef]
19. Craw, D.; Lilly, K. Gold nugget morphology and geochemical environments of nugget formation, southern New Zealand. *Ore Geol. Rev.* **2017**, *79*, 301–315. [CrossRef]

20. Law, S.; Rufaut, C.; Lilly, K.; Craw, D. Geology, evaporative salt accumulation, and geoecology at Springvale historic gold mine, Central Otago, New Zealand. *N. Z. J. Geol. Geophys.* **2016**, *59*, 382–395. [CrossRef]
21. Bennett, E.R.; Youngson, J.H.; Jackson, J.A.; Norris, R.J.; Raisbeck, G.M.; Yiou, F. Combining geomorphic observations with in situ cosmogenic isotope measurements to study anticline growth and fault propagation in Central Otago, New Zealand. *N. Z. J. Geol. Geophys.* **2006**, *49*, 217–231. [CrossRef]
22. Forsyth, P.J. *Geology of the Waitaki Area*; 1:250,000 Geological Map 19; Institute Geological and Nuclear Sciences Limited: Lower Hutt, New Zealand, 2001; 1 sheet, 64p.
23. Youngson, J.H.; Craw, D. Gold nugget growth during tectonically induced sedimentary recycling, Otago, New Zealand. *Sed. Geol.* **1993**, *84*, 71–88. [CrossRef]
24. Craw, D.; Bartle, A.; Fenton, J.; Henderson, S. Lithostratigraphy of gold-bearing Quaternary gravels, middle Manuherikia Valley, Central Otago, New Zealand. *N. Z. J. Geol. Geophys.* **2013**, *56*, 154–170. [CrossRef]
25. Craw, D.; MacKenzie, D.J.; Grieve, P. Supergene gold mobility in orogenic gold deposits, Otago Schist, New Zealand. *N. Z. J. Geol. Geophys.* **2015**, *58*, 123–136. [CrossRef]
26. Craw, D.; MacKenzie, D. *Macraes Orogenic Gold Deposit (New Zealand): Origin and Development of a World Class Gold Mine*; Springer Briefs in World Mineral Deposits; Springer: Berlin, Germany, 2016; 123p, ISBN 978-3-319-35158-2.
27. Craw, D. Placer gold and associated supergene mineralogy at Macraes Flat, East Otago, New Zealand. *N. Z. J. Geol. Geophys.* **2017**, *60*. [CrossRef]
28. Williams, G.J. Economic Geology of New Zealand. *Aust. Inst. Min. Metall. Monog.* **1974**, *4*, 490p.
29. Kerr, G.; Pope, J.; Trumm, D.; Craw, D. Experimental metalloid mobilisation from a New Zealand orogenic gold deposit. *Mine Water Environ.* **2015**, *34*, 404–416. [CrossRef]
30. Kerr, G.; Malloch, K.; Lilly, K.; Craw, D. Diagenetic alteration of a Mesozoic fluvial gold placer deposit, southern New Zealand. *Ore Geol. Rev.* **2016**, *83*, 14–29. [CrossRef]
31. Malloch, K.; Kerr, G.; Craw, D. Placer gold in the Cretaceous Blue Spur Conglomerate at Waitahuna, southern New Zealand. *N. Z. J. Geol. Geophys.* **2017**, *60*, 239–254. [CrossRef]
32. Stewart, J.; Kerr, G.; Prior, D.; Halfpenny, A.; Pearce, M.; Hough, R.; Craw, D. Low temperature recrystallisation of alluvial gold in paleoplacer deposits. *Ore Geol. Rev.* **2017**, *88*, 43–56. [CrossRef]
33. Barker, S.L.L.; Kim, J.P.; Craw, D.; Frew, R.D.; Hunter, K.A. Processes affecting the chemical composition of Blue Lake, an alluvial gold-mine pit lake in New Zealand. *Mar. Freshw. Res.* **2004**, *55*, 201–211. [CrossRef]
34. Craw, D.; Hesson, M.; Kerr, G. Morphological evolution of gold nuggets in proximal sedimentary environments, southern New Zealand. *Ore Geol. Rev.* **2016**, *80*, 784–799. [CrossRef]
35. Dill, H.G.; Wehner, H. The depositional environment and mineralogical and chemical compositions of high ash brown coal resting on early Tertiary saprock, Schirnding Coal Basin, SE Germany. *Int. J. Coal. Geol.* **1999**, *39*, 301–328. [CrossRef]
36. Dill, H.G. Residual clay deposits on basement rocks: The impact of climate and the geological setting on supergene argillitization in the Bohemian Massif (Central Europe) and across the globe. *Earth Sci. Rev.* **2017**, *165*, 1–58. [CrossRef]
37. Tostevin, R.; Craw, D.; van Hale, R.; Vaughan, M. Sources of environmental sulfur in the groundwater system, southern New Zealand. *Appl. Geochem.* **2016**, *70*, 1–16. [CrossRef]
38. Craw, D. Water-rock interaction and acid neutralization in a large schist debris dam, Otago, New Zealand. *Chem. Geol.* **2000**, *171*, 17–32. [CrossRef]
39. Craw, D.; Kerr, G.; Reith, F.; Falconer, D. Pleistocene paleodrainage and placer gold redistribution, western Southland, New Zealand. *N. Z. J. Geol. Geophys.* **2015**, *58*, 137–153. [CrossRef]
40. Rosen, M.; Jones, S. Controls on the chemical composition of groundwater from alluvial aquifers in the Wanaka and Wakatipu basins, Central Otago, New Zealand. *Hydrogeol. J.* **1998**, *6*, 264–281.
41. Jacobson, A.D.; Blum, J.D.; Chamberlain, C.P.; Craw, D.; Koons, P.O. Climatic and tectonic controls on chemical weathering in the New Zealand Southern Alps. *Geochim. Cosmochim. Acta* **2003**, *67*, 29–46. [CrossRef]
42. Dockrey, J.W.; Lindsay, M.B.J.; Mayer, K.U.; Beckie, R.D.; Norlund, K.L.I.; Warren, L.A.; Southam, G. Acidic microenvironments in waste rock characterized by neutral drainage: Bacteria–mineral interactions at sulfide surfaces. *Minerals* **2014**, *4*, 170–190. [CrossRef]
43. Vlassopoulos, D.; Wood, S.A. Gold speciation in natural waters: I. Solubility and hydrolysis reactions of gold in an aqueous solution. *Geochim. Cosmochim. Acta* **1990**, *54*, 3–12. [CrossRef]

44. Usher, A.; McPhail, D.C.; Brugger, J.A. Spectrophotometric study of aqueous Au(III) halide–hydroxide complexes at 25–80 °C. *Geochim. Cosmochim. Acta* **2009**, *73*, 3359–3380. [CrossRef]
45. Nordstrom, D.K.; Southam, G. Geomicrobiology of sulphide mineral oxidation. *Rev. Mineral.* **1997**, *35*, 361–390.
46. Grosse, A.C.; Dicinoski, G.W.; Shaw, M.J.; Haddad, P.R. Leaching and recovery of gold using ammoniacal thiosulphate leach liquors (a review). *Hydrometallurgy* **2003**, *69*, 1–21. [CrossRef]
47. Webster, J.G. The solubility of Au and Ag in the system Au–Ag–S–O_2–H_2O at 25 °C and 1 atm. *Geochim. Cosmochim. Acta* **1986**, *50*, 245–255. [CrossRef]
48. Melashvili, M.; Fleming, C.; Dymov, I.; Matthews, D.; Dreisinger, D. Equation for thiosulphate yield during pyrite oxidation. *Miner. Eng.* **2015**, *74*, 105–111. [CrossRef]
49. Feng, D.; van Deventer, J.S.J. The role of heavy metal ions in gold dissolution in the ammoniacal thiosulphate system. *Hydrometallurgy* **2002**, *64*, 231–246. [CrossRef]
50. Senanyake, G. Review of rate constants for thiosulphate leaching of gold from ores, concentrates and flat surfaces: Effect of host minerals and pH. *Miner. Eng.* **2007**, *20*, 1–15. [CrossRef]
51. Rimstidt, J.D.; Vaughan, D.J. Pyrite oxidation: A state-of-the-art assessment of the reaction mechanism. *Geochim. Cosmochim. Acta* **2003**, *67*, 873–880. [CrossRef]
52. Brierley, C.L. Microbes and supergene deposits: From formation to exploitation. In *Supergene Environments, Processes and Products*; Special Publications of the Society of Economic Geologists; Titley, S.R., Ed.; Society of Economic Geologists: Littleton, CO, USA, 2009; Volume 14, pp. 95–102.